energies

MDPI

Article

Artificial Neural Network Model for Estimating the Pelton Turbine Shaft Power of a Micro-Hydropower Plant under Different Operating Conditions

Raúl R. Delgado-Currín [1,2,*], Williams R. Calderón-Muñoz [2,3,4] and J. C. Elicer-Cortés [2]

[1] Department of Mechanical Engineering, Universidad de La Frontera, Francisco Salazar 01145, Temuco 4811230, Chile
[2] Department of Mechanical Engineering, Universidad de Chile, Beauchef 851, Santiago 8370456, Chile; wicalder@uchile.cl (W.R.C.-M.); jelicer@uchile.cl (J.C.E.-C.)
[3] Center for Sustainable Acceleration of Electromobility-CASE, Universidad de Chile, Beauchef 851, Santiago 8370456, Chile
[4] Energy Center, Universidad de Chile, Beauchef 851, Santiago 8370456, Chile
* Correspondence: raul.delgado@ufrontera.cl

Abstract: The optimal performance of a hydroelectric power plant depends on accurate monitoring and well-functioning sensors for data acquisition. This study proposes the use of artificial neural networks (ANNs) to estimate the Pelton turbine shaft power of a 10 kW micro-hydropower plant. In the event of a failure of the sensor measuring the torque and/or rotational speed of the Pelton turbine shaft, the synthetic turbine shaft power data generated by the ANN will allow the turbine output power to be determined. The experimental data were obtained by varying the operating conditions of the micro-hydropower plant, including the variation of the input power to the electric generator and the variation of the injector opening. These changes consequently affected the flow rate and the pressure head at the turbine inlet. The use of artificial neural networks (ANNs) was deemed appropriate due to their ability to model complex relationships between input and output variables. The ANN structure comprised five input variables, fifteen neurons in a hidden layer and an output variable estimating the Pelton turbine power. During the training phase, algorithms such as Levenberg–Marquardt (L–M), Scaled Conjugate Gradient (SCG) and Bayesian were employed. The results indicated an error of 0.39% with L–M and 7% with SCG, with the latter under high-flow and -energy consumption conditions. This study demonstrates the effectiveness of artificial neural networks (ANNs) trained with the Levenberg–Marquardt (L–M) algorithm in estimating turbine shaft power. This contributes to improved performance and decision making in the event of a torque sensor failure.

Keywords: artificial neural networks; micro-hydropower plant; Pelton turbine; Pelton turbine shaft power

Citation: Delgado-Currín, R.R.; Calderón-Muñoz, W.R.; Elicer-Cortés, J.C. Artificial Neural Network Model for Estimating the Pelton Turbine Shaft Power of a Micro-Hydropower Plant under Different Operating Conditions. *Energies* **2024**, *17*, 3597. https://doi.org/10.3390/en17143597

Academic Editor: Frede Blaabjerg

Received: 11 June 2024
Revised: 5 July 2024
Accepted: 18 July 2024
Published: 22 July 2024

1. Introduction

According to a study by the Harvard Business Review [1], more than 51% of the executives surveyed said they were using artificial intelligence (AI) to improve the quality of their products and 35% said they used it for decision making, which is still consistent today. Despite the fact that, in 2018, AI technologies and expertise were considered too expensive and there was a shortage of experts in the field, in addition to the lack of maturity that existed in those years, this has diminished over time. Today, there is capacity and research that points to a massification in the use of AI in different disciplines, including renewable energies [2,3]. Many hydroelectric plants in South America are decades old, and modernization is a priority for plant operators and grid operators. The need for modernization may include, among other things, improvements in the efficiency, capacity and

safety of existing plants [4]. The application of machine learning for the estimation of critical variables, in conjunction with these enhancements, could result in improvements in their key performance indicators (KPIs). It is essential for the control of a Pelton turbine to have an accurate power estimate [5,6] and predictive maintenance of a micro-hydro power plant [7,8]. However, the traditional physical and statistical models are no longer able to meet the requirements of accuracy, flexibility, speed of construction and training that are demanded by the power plants [7]. There are studies, such as those conducted by Hamid et al. [9], where the estimation of micro-hydroelectric power plant production has been performed using artificial neural network techniques, proving to be effective in forecasting hydroelectric power production under different climate scenarios. Flores et al. [10] present a neural network model to optimize the geometry of hydro turbine blades, utilizing the Levenberg–Marquardt learning algorithm, which successfully predicts efficiency with high accuracy. Arnone's work [11] demonstrates the use of artificial neural networks (ANN) combined with computational fluid dynamics (CFD) to predict the efficiency of a horizontal axis Kaplan turbine, although further validation is suggested to ensure the method's reliability in various scenarios. Yildirim et al. [12] also employ neural networks to predict the performance of micro-hydroelectric power plants. Additional research has explored the application of neural network learning models: Liu et al. [13] propose a Bayesian–Gaussian neural network model to enhance the online prediction capability of hydro turbine systems for control applications in non-linear dynamic systems. Borkowski et al. [14] propose a control system, supported by a neural network and Maximum Power Efficiency Tracking (MEPT) algorithm, to improve the efficiency of variable-speed hydroelectric plants. Ferrero et al. [15] conclude that artificial neural networks (ANNs) applied to hydraulic studies are effective in simulating non-linear behaviors and dynamically predicting water flow, thereby improving accuracy in power production and maintenance. Tan et al. [16] utilize a hybrid algorithm based on social engineering theory and artificial neural networks for fault detection in hydraulic turbines, which is crucial for maintaining the efficiency of hydraulic turbines. Presas et al. [17] investigate the feasibility of predicting dynamic stress in Francis turbines using neural networks (NNs) and stationary sensors, thereby improving predictive maintenance and operational efficiency. Huang et al. [18] present a power prediction model for hydraulic turbines using machine learning, combining gray wolf optimization and support vector machines, achieving good accuracy. Rossi et al. [19] present a general methodology to predict the performance of pumps used as turbines (PATs) using artificial neural networks (ANNs), and the works of Telikani et al. [20] and Yu et al. [21] incorporate artificial neural networks (ANNs) to improve the prediction of pump-as-turbine (PaT) performance. Other research in turbomachinery includes work with neural network models to predict the performance of hydraulic pumps [22] and wind turbines using experimental data from the wind field [23]. Shin et al. [24] review the use of neural networks (NNs) to improve wind energy efficiency, concluding that NNs are effective tools for enhancing efficiency. Finally, it is worth mentioning that current works predict surface hydrocarbons using ensemble neural networks (ENNs) [25] and apply short-term load forecasting to a case study [26], among others.

In this study, neural networks are proposed to estimate the real power output of a Pelton type hydraulic turbine of a 10 kW micro-hydraulic power plant for different operating conditions, where we vary the opening of the turbine injector in four positions. The flow rate is varied every 5 m^3/h in a range from 25 to 120 m^3/h with constant electrical power consumption. The turbine rotation speed is kept constant (200 and 400 rpm). The flow rate is increased for each condition of an electrical load increase (1, 5, 3, 4.5, 6, 6.5 and 9 kW). These experimental data were taken from a previous work (Delgado-Currín et al., 2023 [27]). An artificial neural network is constructed using three machine learning algorithms, L–M, SCG and Bayesian, including estimation error, variance and estimation accuracy.

2. Materials and Methods

2.1. Experimental Model Description

In this study, experiments were conducted to investigate the shaft power of a Pelton turbine on a test bench (as shown in Figure 1) for different nozzle orifices (d), pressure heads (H), discharge flow rates (Q) and different electrical power consumption applied to an electric generator. A Optiflux2000/IFC300 (KROHNE Messtechnik GmbH, Duisburg, Germany) mechanical/electronic flowmeter was used to measure the flow rate, and a Yokogawa EJX11A pitot tube (Yokogawa Electric Corporation, Tokyo, Japan) was used to measure the inlet pressure to the nozzle. The flow rate varies between 25 and 115 m^3/h. The fluid is driven by a KSB Etabloc 80-250 pump (KSB SE & Co. KGaA, Frankenthal, Germany) which circulates the water in a closed circuit; the maximum head and flow rate delivered by the pump are 40 m.c.a and 129.6 m^3/h, respectively. The flow and head of the pump are controlled by an HC 800 variable frequency drive. The pipes of the circuit have a diameter of 4 (in). The Pelton turbine wheel, with a diameter of 240 mm, incorporates 17 buckets installed along its periphery, and the shaft linking the turbine to the electric generator boasts a diameter of 50 mm. A TorqSense torque meter/tachometer (model RWT420) (Sensor Technology Ltd, Banbury, UK) is used to quantify the torque (in N-m) and the speed of the wheel (in rpm). The turbine shaft is complexly connected to a permanent magnet synchronous electric generator, characterized by a power rating of 10 kW, 3-phase AC380V. Various electrical loads are imposed on the electrical generator, ranging from a minimum consumption of 1.5 kW for the three phases (0.5 kW for each phase) to a maximum consumption of 9 kW (3.0 kW for each phase). These electrical loads are generated by electric fan heaters with power ratings of 2 kW and 1 kW, and intermediate power ratings of 1 kW and 0.5 kW, respectively. The voltage and current values for each phase are meticulously measured using Mastech model MS8217 multimeters (Mastech, Hong Kong, China).

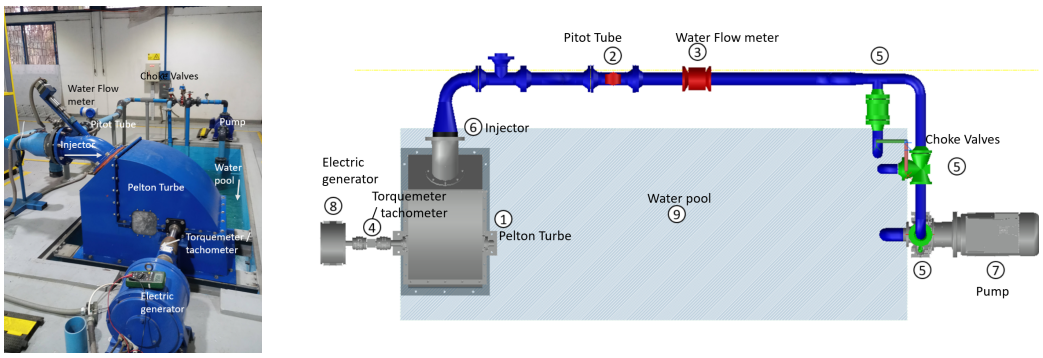

(**a**) (**b**)

Figure 1. (**a**) Installation of a 10 KW micro-hydroelectric power plant and (**b**) sketch of the micro-hydroelectric power plant.

2.2. Operating Conditions of Pressure Head and Electrical Power Consumption

The pressure head operating conditions and electrical power consumption were systematically varied to cover a wide range of scenarios. The pressure head (H), measured at the nozzle inlet, was adjusted with the variable frequency drive to maintain stability at different flow rates. Specifically, the pressure head was varied between 10 m.c.a and 40 m.c.a, ensuring that the system could simulate both low- and high-pressure conditions. As for electrical power consumption, the electrical generator was subjected to various loads to observe turbine performance under different electrical demands. The electrical power consumption was adjusted by connecting electric fan heaters in different configurations, resulting in load increments from 1.5 kW to 9 kW. This configuration allowed the electrical power consumed by the generator to be accurately monitored and measured, facilitating a comprehensive analysis of the shaft power and operating characteristics of the turbine under varying electrical loads.

2.3. Turbine Shaft Power Analysis of the Micro-Hydropower Plant

The equations used to calculate the power of the turbine are presented below [28–32]:

- The brake power generated at the turbine shaft is estimated as

$$P_b = T.\omega \tag{1}$$

where T is the torque of the motor and ω is the angular speed of rotation of the shaft of the turbine. $\omega = \frac{2\pi.N}{60}$.

2.4. Absolute Error

To analyze the accuracy of the Pelton turbine power estimation, the following absolute error equation is used:

$$EA = \left(\frac{|E - P|}{|E|}\right) \times 100 \tag{2}$$

where EA is the absolute error expressed as a percentage, E is the experimental value and P is the estimated value.

2.5. Root Mean Square Error (RMSE)

The Root Mean Square Error (RMSE) is a frequently used measure of the differences between values predicted by a model and the values actually observed. The formula for RMSE is given by

$$\text{RMSE} = \sqrt{\frac{1}{n}\sum_{i=1}^{n}(y_i - \hat{y}_i)^2} \tag{3}$$

where

- n is the number of observations;
- y_i is the actual value;
- $\hat{y}_i$ is the predicted value.

2.6. Coefficient of Determination (R^2)

The Coefficient of Determination (R^2) is a statistical measure that explains how much of the variability in the dependent variable can be explained by the independent variable(s) in a regression model. The formula for R^2 is given by

$$R^2 = 1 - \frac{\sum_{i=1}^{n}(y_i - \hat{y}_i)^2}{\sum_{i=1}^{n}(y_i - \bar{y})^2} \tag{4}$$

where

- n is the number of observations;
- y_i is the actual value;
- $\hat{y}_i$ is the predicted value;
- $\bar{y}$ is the mean of the actual values.

2.7. Artificial Neural Network Model

In the present study, an artificial neural network model for estimating the shaft power of Pelton turbines was developed based on experimental tests [27]. Several factors were considered in the selection of the artificial neural network in this study, such as the architecture of the neural network, the number of hidden layers and the activation function. Regarding the neural network architecture, a recurrent neural network was used because of its ability to capture information from the input data. A single hidden layer architecture was chosen to balance the complexity of the model and to avoid overfitting. The schematic diagram of the ANN model is shown in Figure 2, and the network has three layers: an input layer, a hidden layer and an output layer. The input layer consists of five neurons:

flow rate (m^3/h), pressure (Pa), injector opening, power consumption (kW), pump motor frequency (Hz). The middle layer uses 15 neurons and the output layer is the shaft power.

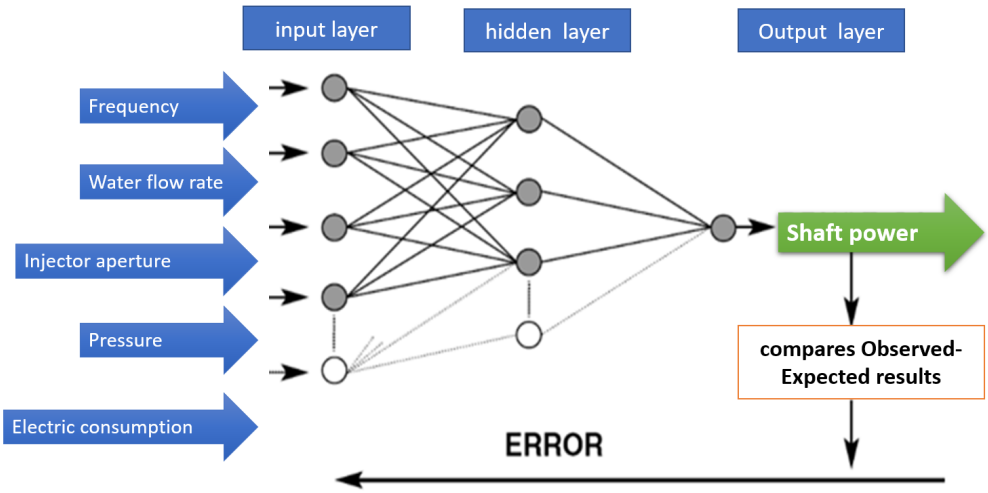

Figure 2. Artificial neural network model used for all three algorithms depicting its architecture with 5 input variables and 1 output variable, which represents a power break.

2.8. Methodology

This study proposes the use of recurrent neural networks to estimate the power output of the Pelton turbine in a 10 kW micro-hydroelectric power plant. Experimental data collected under different operating conditions, such as injector opening, pressure head, water flow rate and electrical power consumption applied to the electrical generator, were used. A flowchart of how the experimental data are obtained and how the flowchart is connected to the neural network is shown in Figure 3. To train the neural network, the data set was divided into a training set and a test set. First, the input and output data were normalized to ensure better convergence during the training of the neural network. We applied three training algorithms in the model and used five input layers and one output layer, as mentioned in the text. Experimental data for training and validation of the neural network model were obtained from experimental trials in the micro-hydroelectric power plant under the following conditions:

1. Variation of the electrical load exerted on the generator (1.5, 3, 4.5, 6, 7.5 and 9 kW of electrical power consumption), as shown in the flow diagram in Figure 3, considering the rotational speed of the turbine-generator shaft as constant. It starts with an injector opening of 25% and a load applied to the generator of 1.5 kW (0.5 kW for each phase), with a shaft speed of 200 rpm. The load is then increased to 3 kW (1 kW per phase) and, in turn, the flow rate is increased to maintain the shaft speed at 200 rpm. This process continues for electrical loads of 4.5, 6, 7.5 and 9 kW. At the end of this test, the system is switched off and then switched on again using the same procedure but with a shaft speed of 400 rpm.
2. Variation of the turbine inlet water flow. We consider an injector opening of 100% and an electrical energy consumption of 9 kW (3 kW for each phase) applied to the electrical generator. We start with a flow rate of 25 m^3/h and then increase the flow rate by 5 m^3/h increments until the maximum allowed flow rate in each test.

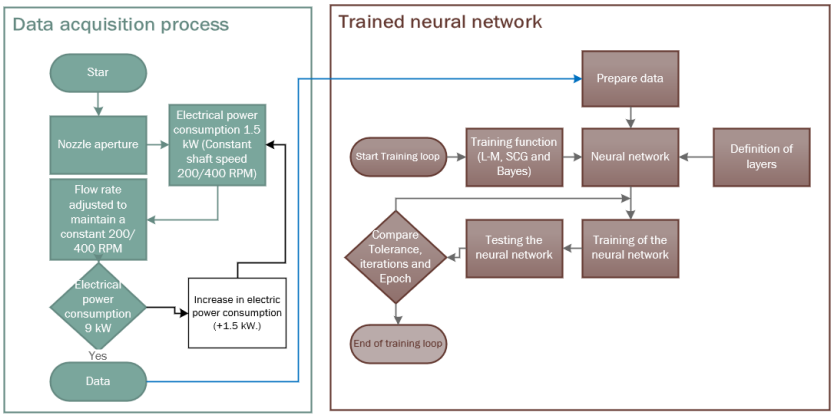

Figure 3. Flowchart of experimental data acquisition and neural network.

2.9. The Training Algorithm and Implementation

The artificial neural network toolbox in MATLAB is used to train and evaluate the [9] neural network using the error backpropagation algorithm. This algorithm adjusts the weights and biases of the network to minimize the error between the estimated output result of the networks and results of the experimental tests. The selection of the artificial neural network used in this study was based on several factors, such as the architecture.

The training data set consisted of 70% of the experimentally collected data, while the remaining 30% was used as a verification set to evaluate the performance of the neural network (15%) and to test the network (15%). Several iterations of the training process were performed to find the best results. Conditions such as a maximum of 100,000 iterations, an estimation tolerance of less than 5% and a minimum number of epochs before convergence of 8 were set beforehand in order to avoid providing low-quality results just by fulfilling these conditions.

2.10. Artificial Neural Network Selection

As for the activation function, the sigmoid activation function was used due to its ability to generate values in the range of 0 to 1, which is suitable for braking power estimation. In addition, the technique of normalizing the input and output data was employed to ensure better convergence during neural network training. Three training algorithms were used: Levenberg–Marquardt backpropagation; Scaled Conjugate Gradient (SCG) and Bayesian.

For the hidden layers, the sigmoid activation function is used, which is commonly used in the hidden layers of neural networks. For the output layer, if no activation function is specified, a linear function is used in regression problems. For these types of problems, it is common to use a linear activation function in the output layer (fitnet); this allows the network to produce continuous outputs without applying any non-linear transformations. The linear function simply passes the weighted sum of the inputs directly as the output of the network.

2.11. Levenberg–Marquardt Algorithm

The Levenberg–Marquardt algorithm is an optimization method used to minimize the cost function during the training of neural networks by adjusting the learning rate and updating the weights at each iteration. The weights are updated by the following equation:

$$w_{k+1} = w_k - \left(J_k^T J_k + \lambda_k I\right)^{-1} J_k^T \nabla C_k \quad (5)$$

where w_k represents the weights at the current iteration, w_{k+1} represents the updated weights at the next iteration, J_k represents the Jacobian matrix evaluated at iteration k, λ_k represents the Levenberg–Marquardt regularization or parameter evaluated at iteration

k, I represents the identity matrix and C_k represents the gradient of the cost evaluated at iteration k.

2.12. Scaled Conjugate Gradient (SCG)

Scaled Conjugate Gradient (SCG) is an optimization method for training neural networks; it uses dynamic learning rates that automatically adjust the weights at each iteration, as calculated by the following equation:

$$\Delta w = -H_k \nabla C_k \tag{6}$$

where Δw represents the change of the proposed weights, H_k represents the approximate inverse Hessian matrix, C_k represents the gradient of the evaluated cost at iteration k and H_k represents the inverse Hessian matrix.

2.13. Neural Networks with Bayesian Learning

The Bayes Net Toolbox for Matlab is a set of tools for working with Bayesian networks in the Matlab environment. It provides structure definition, conditional probability assignment, probabilistic inference, structure and parameter learning based on observational data and statistical analysis. The equation for Bayes' theorem is shown in Equation (7):

$$P(A|B) = \frac{P(B|A) \cdot P(A)}{P(B)} \tag{7}$$

3. Results and Discussion

In Figure 4a, we see that at epoch 29, similar results are obtained between training, validation and testing. Figure 4b shows that the training regression coefficient indicates that the model explains approximately 99.66% of the variability in the training data set. For validation (R = 0.99627), this value indicates that the model explains approximately 99.627% of the variability in the validation data set. A good R in the validation set suggests that the model is not overfitting the training data and generalizes well to unseen data. The result for the test indicates that the model explains approximately 99.657% of the variability in the test data set. Overall the model is able to make a good estimate using completely new data. Moreover, the overall regression tells us that the model is very good at explaining the variation in the full data set.

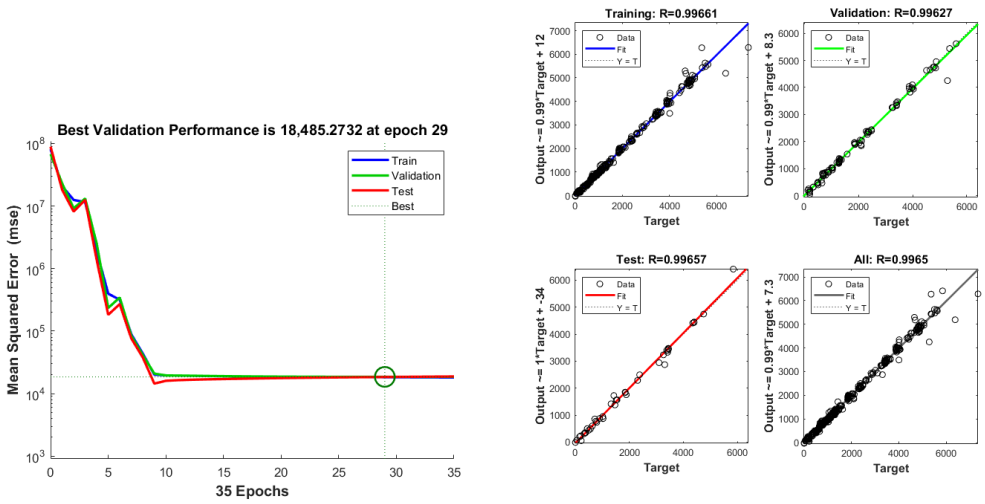

(**a**) (**b**)

Figure 4. (**a**) ANN training performance. (**b**) Regression training, validation and test using the Leverberg–Marquardt training algorithm.

When using the Scale Conjugate Gradient (SCG) training model, it can be seen in Figure 4a that at epoch 82, similar results are achieved for training, validation and testing. Figure 5b shows that the training regression coefficient indicates that the model explains approximately 99.278% of the variability in the training data with a 99.379% training regression coefficient and a 99.00% test regression coefficient.

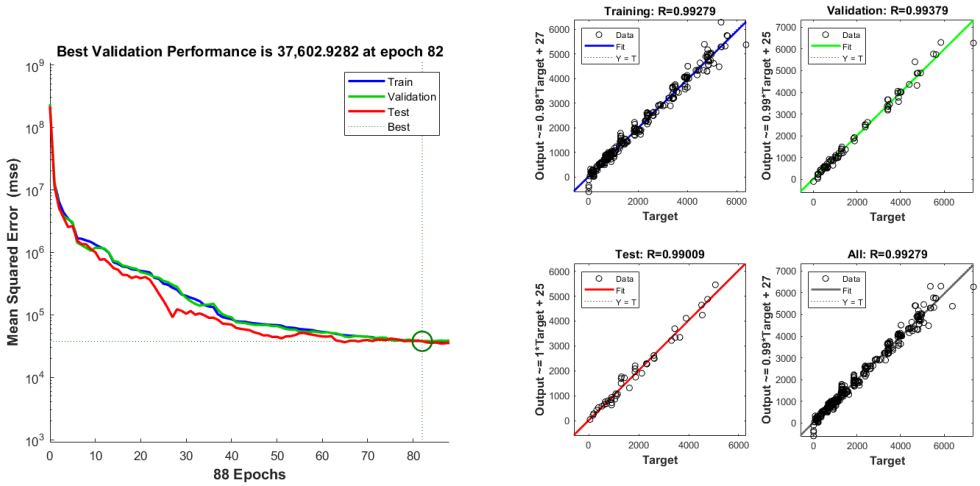

(**a**) (**b**)

Figure 5. (**a**) ANN training performance. (**b**) Regression training, validation and testing using the Scale Conjugate Gradient training model.

Finally, using the Bayesian training algorithm, we can see in Figure 6a that convergence between the test and training data is only achieved at epoch 999. Figure 6b shows that the training regression coefficient was 99.68%, while the test regression coefficient was 99.842%.

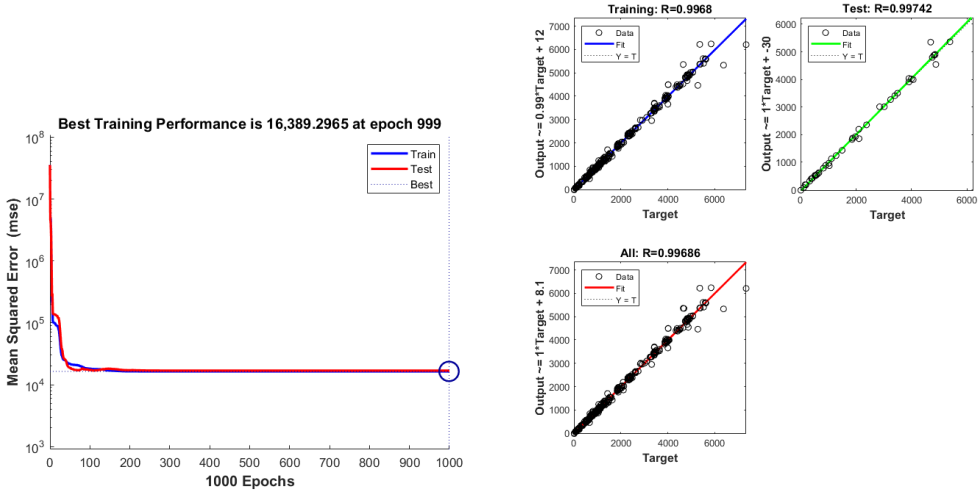

(**a**) (**b**)

Figure 6. (**a**) ANN training performance. (**b**) Regression training, validation and testing using the Bayesian algorithm.

In Figure 7, we can generally highlight that the best training behavior according to the epochs was the Levenberg–Marquardt (L–M) algorithm, seeing a better gradient and lower results during training. This may be an indication that the model most suitable for estimating performance should be the L-M algorithm.

On the other hand, the L–M algorithm showed a low and stable gradient from about epoch 13 onwards. However, for the SGC algorithm, this gradient drop was not very stable, which can also be seen in the failed values of the SGC algorithm (see Figure 7). Finally,

although the Bayesian algorithm is more computationally intensive, requiring 999 epochs to obtain a model, it has a failure rate close to zero, indicating that it would perform well earlier (see Figure 8).

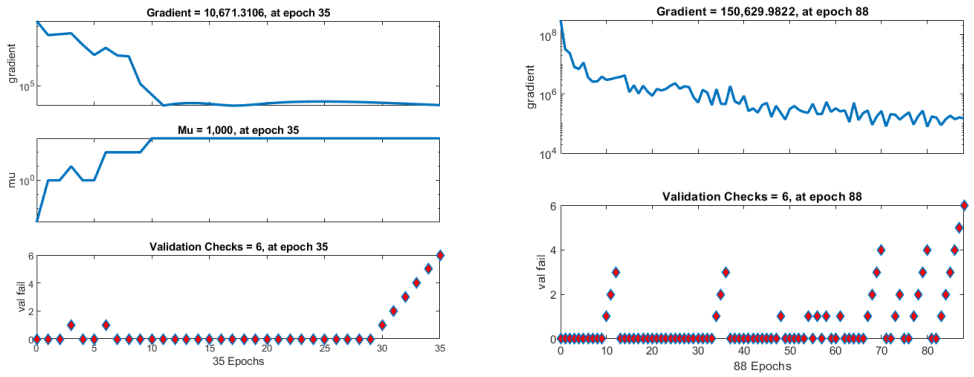

(**a**) (**b**)

Figure 7. (**a**) Training state-of-the-art artificial neural network (ANN) using LM algorithm. (**b**) Training state-of-the-art ANN using SCG algorithm.

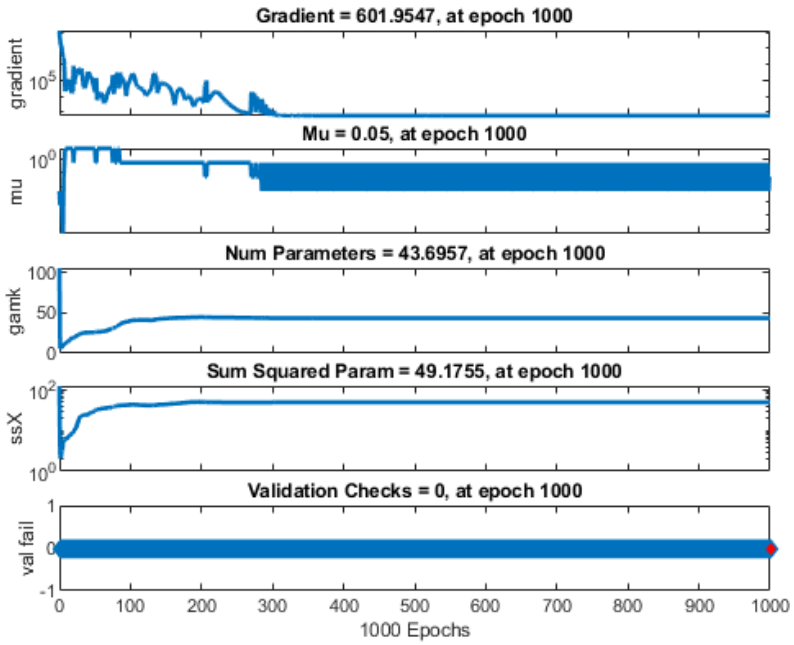

Figure 8. Training state-of-the-art artificial neural network (ANN) using Bayesian algorithm.

3.1. Comparison of Experimental Result with Artificial Neural Network Models: Flow Variation Case

A comparison of the behavior of the three algorithms used in this research (L–M, SCG and Bayesian) was made with the experimental data obtained in a previous work [27], where the variation of the flow rate was considered, taking into account the constant electrical consumption across the electrical generator.

Figure 9a shows the graph of the shaft power at the turbine outlet. Although the three algorithms used seem to perform well in estimating the shaft power, when analyzing the absolute error, which considers the experimental data as real, it is observed that in the section where a flow rate of 25–35 m^3/h is applied, the three training algorithms obtain an error higher than 6%. This means that good results are not obtained when estimating with low shaft power. However, in this range, we can see that the models present a low RMSE, generally below 100 W.

In the flow range of 40–75 m^3/h, a better performance of the three models is observed, with slightly higher estimation accuracy using the Bayesian training algorithm compared to the L–M algorithm, with an error lower than 1%. In this range, the RMSE increases but remains reasonably low considering the increase in shaft power, reflecting that the models maintain good accuracy at moderate flow rates. Finally, in the flow range of 80–95 m^3/h, it is observed that although there is an increase in the error, reaching values of 3–6%, there is a tendency towards the same behavior as the experimental test, with better results obtained using the L–M algorithm. The RMSE increases significantly, reaching up to 800 W, indicating a greater deviation in the predictions in these high flow and power ranges (6000–7000 W). This also reflects that the error variation is proportional to the increase in power. Overall, of the total trials shown in Figure 9a,b, the L–M training algorithm provided better estimates than the other models, and the Bayesian training algorithm provided better estimates than the SCG algorithm. The coefficients of determination (R^2) indicate a good fit of the models in general: SCG with 0.977, L–M with 0.982, and Bayesian with 0.980. The average RMSE values (SCG: 269.5690 W, L–M: 240.2572 W, Bayesian: 252.7586 W) corroborate the accuracy of the models. In summary, although the models are reasonably accurate at low and moderate ranges, their accuracy decreases at high flow rates and powers, suggesting the need for improvements to reduce the error at these high levels.

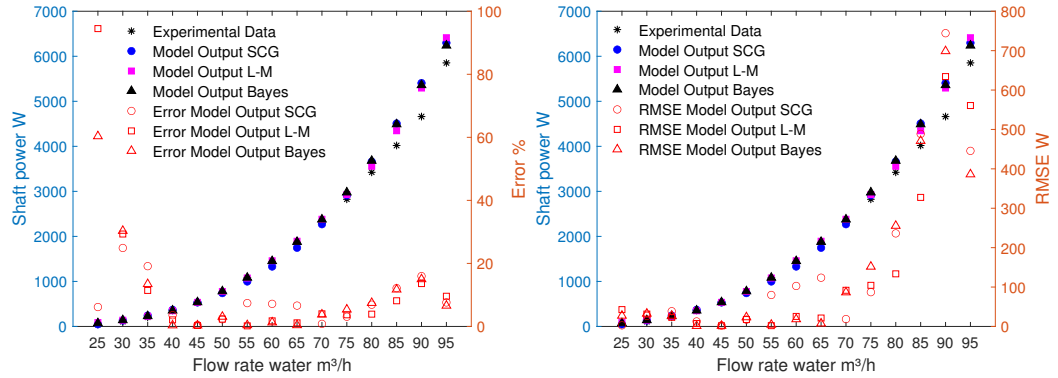

(**a**) (**b**)

Figure 9. Comparison of different power models as a function of flow rate. (**a**) Model-estimated power, real power as a function of flow rate. (**b**) Model-estimated power and real power as a function of flow rate and Root Mean Square Error.

3.2. Comparison of the Experimental Results with the Models of Artificial Neural Networks: Case of Variation of the Consumption of Electricity

A comparison of the behavior of the three algorithms used in this research (L–M, SCG and Bayesian) with the experimental data obtained in a previous work [27] was carried out considering a variable electrical power consumption (1.5, 3, 4.5, 6, 7.5, 9 Kw) applied to an electrical generator, which was connected to the shaft of a Pelton turbine.

In Figure 10, we can see that the graph with the L–M and Bayesian estimation algorithms still has a clear trend in relation to the behavior of the graph with the experimental data, both for low speeds (200 rpm) and for high speeds (400 rpm) of the turbine shaft's rotations. Using the L–M and Bayesian training algorithms gives better power estimation. Figure 11 shows that the highest error in power estimation at the turbine shaft was at an electrical load of 1.5 Kw. For the other electrical power consumption values, the error was considerably lower. As in the previous case, the lowest error was obtained with the L–M and Bayesian models, with minimum error results ranging from 0.46 to 1.83% and maximum values ranging from 1.9 to 4.5 %. In general, the best estimation performance was obtained with the L–M algorithm, which was slightly better than the estimates obtained with the Bayesian training model. On the other hand, and as in the previous case, the SGC algorithm had the highest errors in estimating the experimental turbine power data.

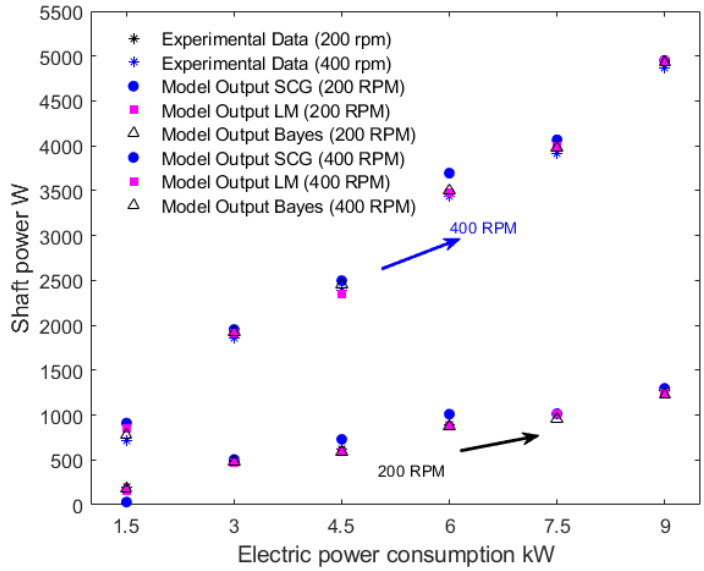

Figure 10. Power estimated by the model and expected power based on power consumption.

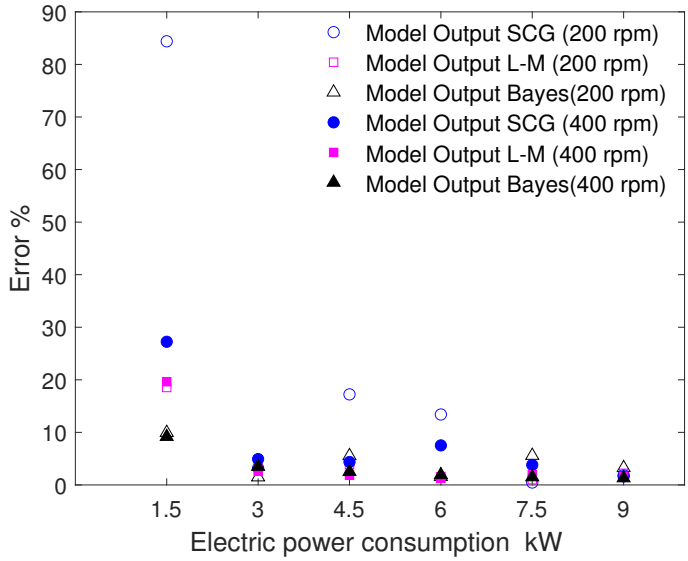

Figure 11. Comparison of absolute error of shaft power estimated by ANN models (SCG, L–M and Bayesian) and experimental data at 200 rpm and 400 rpm as a function of power consumption (kW). RMSE values are shown on the right axis.

Figure 12 shows experimental data and ANN model predictions (SCG, L–M, Bayesian) for shaft power at two speeds (200 and 400 rpm) as a function of power consumption (kW). At low speeds (200 rpm), the models present a low RMSE, indicating accurate predictions. At 400 rpm, although the RMSE increases, reflecting a larger deviation in the predictions, a significant increase in shaft power is also observed. The average RMSE values for the models are SCG: 269.5690 W, L–M: 240.2572 W, and Bayesian: 252.7586 W, while the coefficients of determination (R^2) are SCG: 0.9768, L–M: 0.9816, and Bayesian: 0.9796. Among the models, the performance in terms of the RMSE and fit is best for the L–M model, followed by the Bayesian and SCG algorithms. Experimental data show an increase in shaft power with increasing power consumption, consistent with model predictions, although with greater variations at 400 rpm. In conclusion, the ANN models are accurate at low-load and -speed conditions but need to be improved at high loads and speeds to reduce prediction error, with the L–M model showing the best overall performance.

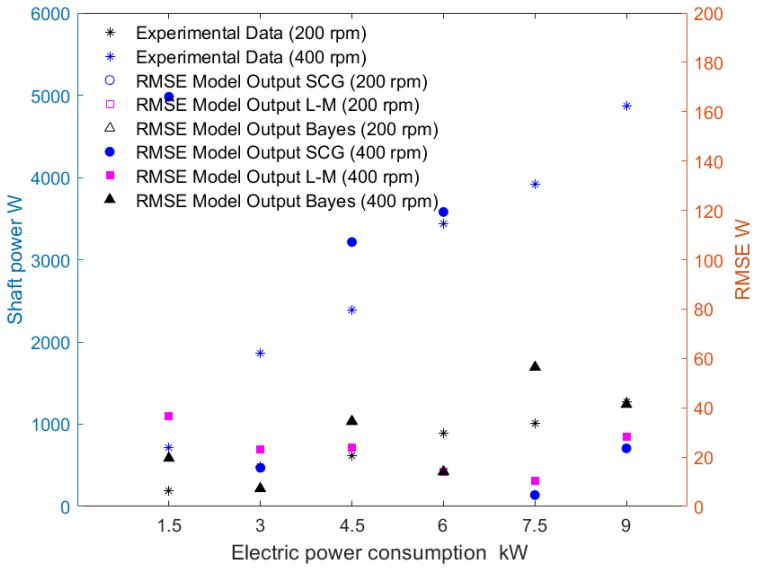

Figure 12. Comparison of RMSE of shaft power estimated by ANN models (SCG, L–M and Bayesian) and experimental data at 200 rpm and 400 rpm as a function of power consumption (kW). RMSE values are shown on the right axis.

4. Conclusions

This work allowed to show the behavior of an artificial neural network using three training algorithms (Levenberg–Marquardt, Scale Conjugate Gradient and Bayesian). The best result in the analysis of the regression coefficient R and failed data of the three models was obtained using the L–M algorithm, followed by the Bayesian algorithm, although the latter has a higher computational cost to train a neural network.

- The results of the turbine power estimation from experimental data show that in the case where we varied the turbine inlet flow rate to change the shaft power, the Levenberg–Marquardt algorithm was the best predictor in terms of accuracy.
- The Levenberg–Marquardt training algorithm slightly outperformed the Bayesian inference model in terms of estimating the turbine output power results when varying the electrical load applied to the electrical generator connected to the turbine.

Overall, the Levenberg–Marquardt algorithm achieved a higher accuracy in estimating the Pelton turbine power output from experimental tests under different operating conditions, as measured using absolute error, RMSE and R^2.

Author Contributions: Conceptualization, R.R.D.-C., W.R.C.-M. and J.C.E.-C.; formal analysis, R.R.D.-C. and W.R.C.-M.; investigation, R.R.D.-C.; methodology, R.R.D.-C. and W.R.C.-M.; project administration, W.R.C.-M. and J.C.E.-C.; resources, W.R.C.-M. and J.C.E.-C.; software (Matlab R2022b-academic), R.R.D.-C.; supervision, W.R.C.-M.; validation, R.R.D.-C. and W.R.C.-M.; visualization, R.R.D.-C. and W.R.C.-M.; writing—original draft preparation, R.R.D.-C.; writing—review and editing, R.R.D.-C. and W.R.C.-M. All authors have read and agreed to the published version of the manuscript.

Funding: This research received no external funding.

Data Availability Statement: The raw data and neural network models supporting the conclusions of this article will be made available by the authors upon request.

Acknowledgments: The authors would like to thank the Fabrication Laboratory of the Department of Mechanical Engineering for their assistance with the experimental setup.

Conflicts of Interest: The authors declare no conflicts of interest.

Abbreviations

The following abbreviations are used in this manuscript:

ANN	Artificial Neural Network
L–M	Levenberg–Marquardt
SCG	Scaled Conjugate Gradient

References

1. Davenport, T.H.; Ronanki, R. Artificial intelligence for the real world. *Harv. Bus. Rev.* **2018**, *96*, 108–116.
2. Shoaei, M.; Noorollahi, Y.; Hajinezhad, A.; Moosavian, S.F. A review of the applications of artificial intelligence in renewable energy systems: An approach-based study. *Energy Convers. Manag.* **2024**, *306*, 118207. [CrossRef]
3. Yousef, L.A.; Yousef, H.; Rocha-Meneses, L. Artificial Intelligence for Management of Variable Renewable Energy Systems: A Review of Current Status and Future Directions. *Energies* **2023**, *16*, 8057. [CrossRef]
4. IHA. *Hydropower Status Report: Sector Trends and Insights*; IHA: London, UK, 2018.
5. Díaz, G.; Sen, M.; Yang, K.; McClain, R.L. Dynamic prediction and control of heat exchangers using artificial neural networks. *Int. J. Heat Mass Transf.* **2001**, *44*, 1671–1679. [CrossRef]
6. Ohana, I.; Bezerra, U.; Vieira, J. Data-mining experiments on a hydroelectric power plant. *IET Gener. Transm. Distrib.* **2012**, *6*, 395–403. [CrossRef]
7. Betti, A.; Crisostomi, E.; Paolinelli, G.; Piazzi, A.; Ruffini, F.; Tucci, M. Condition monitoring and predictive maintenance methodologies for hydropower plants equipment. *Renew. Energy* **2021**, *171*, 246–253. [CrossRef]
8. Rutagarama, M. Deep Learning for Predictive Maintenance in Impoundment Hydropower Plants. Ph.D. Thesis, Ecole Polytechnique Fédérale de Lausanne Écublens, Lausanne, Switzerland, 2019.
9. Hammid, A.T.; Sulaiman, M.H.B.; Abdalla, A.N. Prediction of small hydropower plant power production in Himreen Lake dam (HLD) using artificial neural network. *Alex. Eng. J.* **2018**, *57*, 211–221. [CrossRef]
10. Flores, J.; Hernandez, J.; Urquiza, G. Numerical optimization of the hydraulic turbine runner blades applying neuronal networks. In Proceedings of the Electronics, Robotics and Automotive Mechanics Conference (CERMA'06), Cuernavaca, México, 26–29 September 2006; Volume 2, pp. 194–199.
11. Arnone, A.; Marconcini, M.; Rubechini, F.; Schneider, A.; Alba, G. Kaplan turbine performance prediction using CFD: An artificial neural network approach. In Proceedings of the Proceedings of the Conference HYDRO 2009, Lyon, France, 26–28 October 2009.
12. Yildirim, S.; Bingol, M.S.; Cil, M. Performance Analysis of Pelton Turbines Using Proposed Neural Network Predictors. In Proceedings of the International Conference on Computational Methods in Applied Sciences Istanbul, Turkey, 12–16 July 2019.
13. Liu, Y.J.; Fang, Y.J.; Zhu, X.M. Modeling of hydraulic turbine systems based on a Bayesian–Gaussian neural network driven by sliding window data. *J. Zhejiang Univ. Sci.* **2010**, *11*, 56–62. [CrossRef]
14. Borkowski, D. Maximum efficiency point tracking (MEPT) for variable speed small hydropower plant with neural network based estimation of turbine discharge. *IEEE Trans. Energy Convers.* **2017**, *32*, 1090–1098. [CrossRef]
15. Ferrero Bermejo, J.; Gómez Fernández, J.F.; Olivencia Polo, F.; Crespo Márquez, A. A review of the use of artificial neural network models for energy and reliability prediction. A study of the solar PV, hydraulic and wind energy sources. *Appl. Sci.* **2019**, *9*, 1844. [CrossRef]
16. Tan, Y.; Zhan, C.; Pi, Y.; Zhang, C.; Song, J.; Chen, Y.; Golmohammadi, A.M. A Hybrid Algorithm Based on Social Engineering and Artificial Neural Network for Fault Warning Detection in Hydraulic Turbines. *Mathematics* **2023**, *11*, 2274. [CrossRef]
17. Presas, A.; Valentin, D.; Zhao, W.; Egusquiza, M.; Valero, C.; Egusquiza, E. On the use of neural networks for dynamic stress prediction in Francis turbines by means of stationary sensors. *Renew. Energy* **2021**, *170*, 652–660. [CrossRef]
18. Huang, X.; Lu, Q.; Zhou, H.; Huang, W.; Wang, S. Study on hydroturbine power trend prediction based on machine learning. *Energy Rep.* **2023**, *10*, 1996–2005. [CrossRef]
19. Rossi, M.; Renzi, M. A general methodology for performance prediction of pumps-as-turbines using Artificial Neural Networks. *Renew. Energy* **2018**, *128*, 265–274. [CrossRef]
20. Telikani, A.; Rossi, M.; Khajehali, N.; Renzi, M. Pumps-as-Turbines' (PaTs) performance prediction improvement using evolutionary artificial neural networks. *Appl. Energy* **2023**, *330*, 120316. [CrossRef]
21. Yu, W.; Zhou, P.; Miao, Z.; Zhao, H.; Mou, J.; Zhou, W. Energy performance prediction of pump as turbine (PAT) based on PIWOA-BP neural network. *Renew. Energy* **2024**, *222*, 119873. [CrossRef]
22. Balacco, G. Performance prediction of a pump as turbine: Sensitivity analysis based on artificial neural networks and evolutionary polynomial regression. *Energies* **2018**, *11*, 3497. [CrossRef]
23. Sun, H.; Qiu, C.; Lu, L.; Gao, X.; Chen, J.; Yang, H. Wind turbine power modelling and optimization using artificial neural network with wind field experimental data. *Appl. Energy* **2020**, *280*, 115880. [CrossRef]
24. Shin, H.; Rüttgers, M.; Lee, S. Neural networks for improving wind power efficiency: A review. *Fluids* **2022**, *7*, 367. [CrossRef]
25. Wang, F.; Chen, D.; Li, M.; Chen, Z.; Wang, Q.; Jiang, M.; Rong, L.; Wang, Y.; Li, S.; Iltaf, K.H.; et al. A novel method for predicting shallow hydrocarbon accumulation based on source-fault-sand (S-F-Sd) evaluation and ensemble neural network (ENN). *Appl. Energy* **2024**, *359*, 122684. [CrossRef]

26. Morais, L.B.S.; Aquila, G.; de Faria, V.A.D.; Lima, L.M.M.; Lima, J.W.M.; de Queiroz, A.R. Short-term load forecasting using neural networks and global climate models: An application to a large-scale electrical power system. *Appl. Energy* **2023**, *348*, 121439. [CrossRef]
27. Delgado-Currín, R.; Calderón-Muñoz, W.; Elicer-Cortés, J.C. Experimental study of the performance of a Pelton turbine of a micro power plant for different operating conditions. *Eng. Res.* **2023**, *3*, 2–11.
28. Rafae Alomar, O.; Maher Abd, H.; Mohamed Salih, M.M.; Aziz Ali, F. Performance analysis of Pelton turbine under different operating conditions: An experimental study. *Ain Shams Eng. J.* **2022**, *13*, 101684. [CrossRef]
29. Cobb, B.R.; Sharp, K.V. Impulse (Turgo and Pelton) turbine performance characteristics and their impact on pico-hydro installations. *Renew. Energy* **2013**, *50*, 959–964. [CrossRef]
30. Stamatelos, F.; Anagnostopoulos, J.; Papantonis, D. Performance measurements on a Pelton turbine model. *Proc. Inst. Mech. Eng. Part J. Power Energy* **2011**, *225*, 351–362. [CrossRef]
31. Gupta, V.; Khare, R.; Prasad, V. Performance evaluation of Pelton turbine: A review. *Hydro Nepal Water Energy Env.* **2013**, *13*, 28–35. [CrossRef]
32. Kumar, K.; Saini, R. A review on operation and maintenance of hydropower plants. *Sustain. Energy Technol. Assess.* **2022**, *49*, 101704. [CrossRef]